

# Exploring Human-in-the-Loop Test-Time Adaptation by Synergizing Active Learning and Model Selection

Yushu Li<sup>1,2\*</sup>  
eeyushuli@mail.scut.edu.cn

Yongyi Su<sup>1,2\*</sup>  
eesuyongyi@mail.scut.edu.cn

Xulei Yang<sup>2</sup>  
yangx@i2r.a-star.edu.sg

Kui Jia<sup>3</sup>  
kuijia@cuhk.edu.cn

Xun Xu<sup>2†</sup>  
alex.xun.xu@gmail.com

<sup>1</sup> South China University of Technology,  
Guangzhou, China

<sup>2</sup> Institute for Infocomm Research,  
A\*STAR,  
Singapore

<sup>3</sup> School of Data Science,  
The Chinese University of Hong Kong,  
Shenzhen, China

## Abstract

Existing test-time adaptation (TTA) approaches often adapt models with the unlabeled testing data stream. A recent attempt relaxed the assumption by introducing limited human annotation, referred to as Human-In-the-Loop Test-Time Adaptation (HILTTA) in this study. The focus of existing HILTTA lies on selecting the most informative samples to label, a.k.a. active learning. In this work, we are motivated by a pitfall of TTA, i.e. sensitive to hyper-parameters, and propose to approach HILTTA by synergizing active learning and model selection. Specifically, we first select samples for human annotation (active learning) and then use the labeled data to select optimal hyper-parameters (model selection). A sample selection strategy is tailored for choosing samples by considering the balance between active learning and model selection purposes. We demonstrate on 4 TTA datasets that the proposed HILTTA approach is compatible with off-the-shelf TTA methods which outperform the state-of-the-art HILTTA methods and stream-based active learning methods. Importantly, our proposed method can always prevent choosing the worst hyper-parameters on all off-the-shelf TTA methods. The source code will be released upon publication.

## 1 Introduction

The disparity in distribution between training and testing data leads to poor generalization of deep neural networks. The data distribution of testing data is often unknown until the inference stage [40, 41] and the distribution may experience constant shift [19, 32, 33, 42, 46]. These practical challenges lead to the research into test-time adaptation (TTA) [37, 38,

\* Equal contribution.

† Correspondence to Xun Xu: alex.xun.xu@gmail.com.

© 2024. The copyright of this document resides with its authors.

It may be distributed unchanged freely in print or electronic forms.

[40], [41], [42]. Despite achieving impressive results on a wide range of tasks, e.g. classification [40], image segmentation [43] and object detection [9], the fully unsupervised TTA paradigm is still overwhelmed by remaining challenges including hyper-parameter tuning [48], continual distribution shift [42], non-i.i.d. [9, 80, 46], class imbalance [58], etc. Unfortunately, there are still no principled solutions to address these challenges without relaxing the assumptions.

Recently, efforts have been made to the exploration of introducing a limited annotation budget during test-time adaptation (SimATTA) [10], also referred to as human-in-the-loop test-time adaptation (HILTITA) throughout this study. SimATTA [10] demonstrated that adapting pre-trained models with labeled testing data could substantially improve the effectiveness and prevent catastrophic forgetting [15, 20].

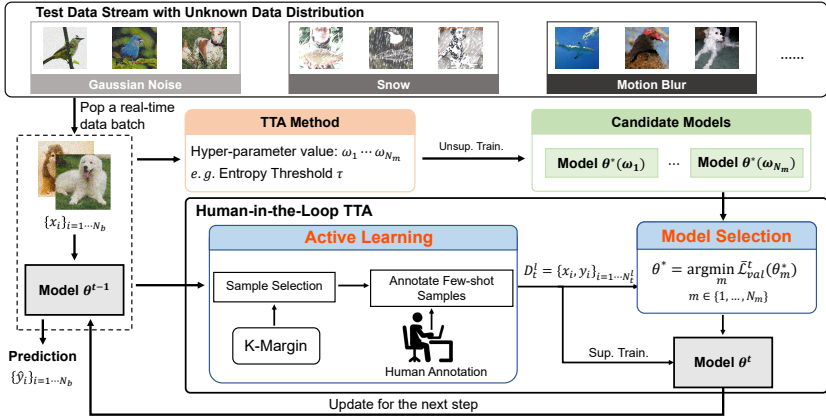


Figure 1: An illustration of Human-in-the-Loop Test-Time Adaptation framework. Upon collecting a batch of testing data  $\{x_i\}_{i=1 \dots N_b}$ , we train multiple candidate models  $\theta^*(\omega_m)$  using candidate hyper-parameters  $\{\omega_m\}$ . We further select candidate samples for annotation through K-Margin. Model selection is achieved by choosing the hyper-parameter minimizing validation objective. We repeat until testing data stream terminates.

Although theoretically guaranteed and offering superior results, the current implementation of the HILTITA method adheres to the conventional path of research in active learning [54, 55]. In this study, we aim to explore the question: **How can human-in-the-loop test-time adaptation be realized beyond an active learning perspective?** To answer this question, we first revisit the pitfalls of state-of-the-art test-time adaptation [48]. Among the multiple remaining pitfalls, we pinpoint hyper-parameter selection as the most nasty one due to the high risk of selecting inappropriate hyper-parameters by many TTA methods. Therefore, we offer a fresh perspective on human-in-the-loop test-time adaptation by synergizing active learning and model selection.

In specific, upon observing a testing sample, the model will first make an instant prediction to minimize inference latency. When a fixed number of testing samples are observed, we employ a data selection strategy to recommend a subset of testing samples for annotation. The labeled data will then be utilized as the validation set for selecting the best hyper-parameters. Finally, the model is further updated with the labeled data in a fully supervised fashion. We argue that the computation cost will not significantly increase by the introduced model selection procedure, especially compared with the time required for human labeling.

To enable the novel HILTITA procedure, we identify two major challenges. First, the

validation objective deserves delicate design due to the small validation set. Without seeing the whole picture of testing data, a naive model selection strategy may overfit to the labeled testing data within a local time window. Second, the data selection strategy must be well-calibrated for HILTТА. Employing the data acquisition functions solely developed for either active learning [65] or active testing [47] is suboptimal.

To tackle these challenges, we first propose a hyper-parameter regularization technique by considering the deviation of model predictions from a frozen source model. We further combine the ranking scores of validation loss and the deviation as the scoring function for model selection. To accommodate the data selection strategy for HILTТА synergizing active learning and model selection, we prioritize both model uncertainty and sample diversity through a simple re-weighting. We summarize the contributions of this work as follows.

- We approach Human-In-the-Loop Test-Time Adaptation (HILTТА) by synergizing active learning and model selection.
- To prevent the model selection from overfitting to a small validation set and local distribution, we introduce multiple regularization techniques. We further identify an effective selection strategy for HILTТА by considering the feature diversity and model uncertainty.
- We demonstrate that the proposed method is compatible with state-of-the-art off-the-shelf TТА methods. The combined methods outperform dedicated active TТА method and stream-based active learning method on four test-time adaptation datasets.

## 2 Related Work

**Test-Time Adaptation:** Traditional approaches towards unsupervised domain adaptation (UDA) learns indiscriminative features. Simultaneously training on both source and target domain data is often infeasible due to privacy issues or storage overhead. Source-free domain adaptation (SFDA) tackles this issue and adapts model weights to target domain data only [22, 23, 25, 45]. In contrast, test-time adaptation (TTA) emerges in response to adapting to an unknown target domain at the inference stage [20, 57, 40, 41, 42]. The success of prevailing TТА methods owns to self-training on unlabeled testing data. To prevent the model from being misled by incorrect pseudo labels, a.k.a. confirmation bias [4], TТА is achieved by partial model weights update [14, 44], adding regularization [25, 38] and pseudo label thresholding [30, 39]. Nevertheless, existing approaches are mainly built upon a fully unsupervised adaptation protocol. We argue that sparse human annotation budgets might be available and exploiting annotation budget in TТА, referred to as human-in-the-loop TТА, has gained attention from the community [40]. Contrary to the traditional active learning perspective [40], we identified an unexplored opportunity to treat labeled data as the validation set for model selection and we propose a novel HILTТА paradigm by synergizing active learning and model selection.

**Active Learning:** Active learning (AL) aims to select the most informative samples for Oracle to label for supervised training. Prevailing approaches often prioritize uncertainty [2], feature diversity [65] or the combination of both [2]. The traditional AL approaches often adopt a batch-wise paradigm. When data arrive in a sequential manner stream-based AL [64] proposed to quantify the increment of the determinant as the criteria for incremental sample selection. Active learning was integrated into test-time adaptation to tackle the forgetting issue [40]. In contrast to tackling HILTТА from a pure active learning perspective, we propose to synergize active learning and model selection. Selecting samples for model selection

often relies on an orthogonal objective to active learning. In the related works, active testing [14, 17] was developed to select a subset of testing data that is representative of the whole testing data. Active testing has been demonstrated to help label-efficient model validation. Nevertheless, active learning and active testing will prioritise supervised training and model validation respectively. We believe either is not enough for the purpose of synergizing active learning and model selection for test-time adaptation.

### 3 Methodology

#### 3.1 Human-in-the-Loop Test-Time Adaptation protocol

We first provide an overview of the existing test-time adaptation (TTA) evaluation protocol. TTA aims to adapt a pre-trained model  $h(x; \theta)$  to a target testing data stream  $D = \{x_i, \bar{y}_i\}_{i=1 \dots N_t}$  where  $x_i$  and  $\bar{y}_i \in \{1 \dots C\}$  denote the testing sample and the associated unknown label, respectively. Existing test-time adaptation approaches often make an instant prediction  $\hat{y} = h(x; \theta)$  on each testing sample and then update model weights  $\theta$  upon observing a cumulative batch of samples  $B_t = \{x_i\}_{i=1 \dots N_b}$  where  $t$  refers to the  $t$ -th minibatch. Prevailing methods enable adaptation by self-training [39, 41] or distribution alignment [57]. Unlike the existing assumption of totally unsupervised adaptation, additional human annotation  $B_t^l = \{x_j, y_j\}_{j=1 \dots N_b^l}$  within each batch could be introduced [10] and TTA is implemented on the combine of large unlabeled data  $B_t^u = B_t \setminus B_t^l$  and sparsely labeled data  $B_t^l$ . We refer to the novel evaluation protocol as Human-in-the-Loop Test-Time Adaptation (HILTTA) throughout the study.

#### 3.2 Model Selection with Sparse Annotation

We present the details for model selection with sparse human annotation on the testing data stream. The choice of hyper-parameters is known to have a significant impact on the performance of model training and generalization. W.l.o.g., we define the task of model selection by introducing a fixed candidate pool of hyper-parameters  $\Omega = \{\omega_m\}_{m=1 \dots N_m}$  with  $N_m$  options. The choice of hyper-parameters hinges on the sensitivity of respective TTA methods, e.g. pseudo label threshold, learning rate, and loss coefficient are commonly chosen hyper-parameters for selection. We further denote the discriminative model trained upon the hyper-parameters  $\omega$  as  $\theta(\omega)$ . The model selection can be formulated as a bi-level optimization problem as follows, where  $\mathcal{L}_{tr}(\cdot; \omega)$  denotes the training loss dictated by the hyper-parameter  $\omega$ ,  $\mathcal{L}_{val}(\cdot, \cdot)$  denotes the validation loss/objective and  $D^l$  refers to the labeled data.

$$\min_{\omega \in \Omega} \frac{1}{N_t^l} \sum_{x_j, y_j \in D^l} \mathcal{L}_{val}(h(x_j; \theta^*(\omega)), y_j) \quad s.t. \quad \theta^*(\omega) = \arg \min_{\theta} \frac{1}{N_t} \sum_{x_i \in D} \mathcal{L}_{tr}(h(x_i); \omega) \quad (1)$$

We interpret the above bi-level optimization problem as discovering the optimal hyper-parameter  $\omega$  trained upon which the model weights  $\theta^*$  achieves the best performance on the labeled dataset. Solving the above problem through gradient-based method [24] is infeasible for TTA tasks where adaptation speed is a major concern while gradient-based methods require iteratively updating between meta gradient descent  $\nabla_{\omega} \mathcal{L}_{val}$  and task gradient descent  $\nabla_{\theta} \mathcal{L}_{tr}$ . Considering the task gradient descent only takes a few steps in a typical TTA setting, we opt for an exhaustive search for the hyper-parameters in the discretized hyper-parameter space. In specific, we enumerate the candidate models adapted with different hyper-parameters as  $\{\theta_m^*\}_{m=1 \dots |\Omega|}$ . The candidate with the best validation loss is chosen as the best model  $\theta^*$ , as follows.

$$\forall m = 1 \dots N_m, \quad \theta_m^* = \arg \min_{\theta} \frac{1}{N_t} \sum_{x_i \in D} \mathcal{L}_{tr}(h(x_i); \omega_m) \quad \theta^* = \arg \min_{\theta \in \{\theta_m^*\}} \sum_{x_j, y_j \in D^l} \mathcal{L}_{val}(h(x_j; \theta), y_j) \quad (2)$$

The specific choice of training loss  $\mathcal{L}_{tr}$  could be arbitrary off-the-shelf test-time adaptation methods while the design of validation loss  $\mathcal{L}_{val}$  deserves careful attention in order to achieve robust model selection.

### 3.3 Design of Validation Objective

In this section, we take into consideration two principles for the construction of validation objectives. First, the validation loss should mimic the behaviour of the model on the testing data stream. Assuming the limited labeled data takes a snapshot of the whole testing data stream and classification is the task to be addressed, an intuitive choice is the cross-entropy loss as follows.

$$\mathcal{H}_{ce}(x_i; \theta_m^*) = \sum_{c=1 \dots C} \mathbb{1}(y_i = c) \log h_c(x_i; \theta_m^*) \quad (3)$$

Alternative to the continuous cross-entropy loss, accuracy also characterizes the performance on the labeled validation set. However, the discretized nature of accuracy renders this option less suitable due to many tied optimal hyper-parameters.

**Regularization for Stable Model Selection:** The stability of model selection heavily depends on the selection of validation set and the variation of target domain distribution. Under a more realistic TTA scenario, the target domain distribution could shift over time, e.g. the continual test-time adaptation [42]. Such a realistic challenge may render cross-entropy loss less effective due to over-adapting to a local distribution. To stabilize the model selection procedure, we propose the following two measures.

**Anchor Deviation for Regularizing Model Selection:** We first introduce an anchor deviation to regularize the model selection procedure. This regularization is similar to the anchor network proposed in [38] except that we use the anchor deviation to regularize model selection which is orthogonal to the purpose in [38]. Specifically, we keep a frozen source domain model, denoted as  $\theta_0$ . The anchor loss is defined as the L2 distance between the posteriors of the frozen source model and the  $m$ -th candidate model  $\theta_m^*$ . A big deviation from the source model prediction suggests the model has been adapted to a very specific target domain and further adapting towards one direction would increase the risk of failing to adapt to the continually changing distribution.

$$\mathcal{R}_{anc}(x_i; \theta_m^*) = \frac{1}{N_b} \sum_{x_i, y_i \in D^I} \|h(x_i; \theta_0) - h(x_i; \theta_m^*)\| \quad (4)$$

**Smoothed Scoring for Model Selection:** To determine the optimal model to select, we combine the cross-entropy loss and the anchor deviation as the final score. Direct summing the two metrics as the model selection score is sub-optimal due to the relative scale between the two metrics. Therefore, we propose to first normalize the two metrics. After the normalization, the relative size relationships of different candidate model scores are preserved, and a comparable validation loss can be conveniently obtained by addition, as below.

$$\begin{aligned} \forall m = 1 \dots |\Omega|, \quad \text{Norm}(x) &= (x - \min(x)) / (\max(x) - \min(x)), \quad S_{ce}(x_i; \theta_m^*) = \text{Norm}(\mathcal{H}_{ce}(x_i; \theta_m^*)) \\ S_{anc}(x_i; \theta_m^*) &= \text{Norm}(\mathcal{R}_{anc}(x_i; \theta_m^*)), \quad \mathcal{L}_{val}(x_i; \theta_m^*) = S_{ce}(x_i; \theta_m^*) + S_{anc}(x_i; \theta_m^*) \end{aligned} \quad (5)$$

Considering that testing data stream is often highly correlated, i.e. temporally adjacent samples are likely subject to the same distribution shift, the optimal hyper-parameter/model should change smoothly as well. To encourage a smooth transition of the optimal model, we select the optimal model following an exponential moving average fashion as in Eq. 6 where we denote the moving average validation loss at the  $t$ -th batch as  $\tilde{\mathcal{L}}_{val}^t$ .

$$\tilde{\mathcal{L}}_{val}^t(\theta_m^*) = \beta \tilde{\mathcal{L}}_{val}^{t-1}(\theta_m^*) + (1 - \beta) \frac{1}{|B_t^I|} \sum_{x_j, y_j \in B_t^I} \mathcal{L}_{val}(h(x_j; \theta_m^*), y_j), \quad \theta^* = \arg \min_m \tilde{\mathcal{L}}_{val}^t(\theta_m^*) \quad (6)$$

### 3.4 Sample Selection for HILTTA

The sample selection strategy should balance the objectives of active learning and model selection for more effective HILTTA. We achieve this target from two perspectives. First, the selected samples should prioritize low-confidence samples for more effective active learning, as adopted by SimATTA [10] through incremental K-means. However, selecting redundant low-confidence samples may harm the effectiveness of model validation. This motivates us to select samples approximating the testing data distribution, similar to the objective of active testing [16]. Biasing towards either criterion would result in suboptimal HILTTA.

The above objectives could be achieved by a recent active learning approach, BADGE [8], which takes the gradient of loss w.r.t. the penultimate layer feature as the uncertainty weighted feature as  $g_x = \frac{\partial}{\partial \theta_{out}} \mathcal{L}_{ce}(h(x; \theta), \hat{y})$ , on which K-Means++ is applied for active selection. The feature dimension is the product of the number of classes  $C$  and penultimate layer channels  $D$ , i.e.  $g_x \in \mathbb{R}^{C \times D}$ . Accumulating the feature over all categories results in overly high dimension features for large-scale classification tasks, e.g.  $C = 1000$  for ImageNet [9]. To mitigate the ultra-high dimension challenge, we integrate uncertainty into feature representation by multiplying the uncertainty, measured by the margin confidence, to the feature representation as in Eq. 7, where  $\text{sort}^d$  refers to the descending sorting.

$$\hat{p} = \text{sort}^d[h_1(x_i; \theta), h_2(x_i; \theta), \dots, h_C(x_i; \theta)], \quad g_i = (1 - \hat{p}_1 + \hat{p}_2)f(x_i; \theta) \quad (7)$$

The above design prioritizes the difference between the probability of the most confident and second most confident classes as a quantification of model uncertainty.

**Sample Selection via K-Margin:** The samples to be selected for annotation are eventually obtained by conducting a K-Center clustering on the uncertainty-weighted features within each minibatch, as in Eq. 8, which is referred to as K-Margin clustering. We select  $K$  samples  $B_t^l$  such that the maximal distance of all testing sample embedding is minimized. We deliberately exclude the selected samples in the previous minibatch, as opposed to SimATTA [10], because the labeled samples will serve as the validation set, and excluding new samples that may overlap with previously selected samples could undermine the effectiveness of model selection. The following problem can be solved via a greedy selection algorithm [65].

$$\min_{B_t^l \subseteq \{g_i\}_{i=1}^{N_b}} \max_{g_i \in \{g_i\}_{i=1}^{N_b}} \min_{c_k \in B_t^l} \|g_i - c_k\|, \quad s.t. |B_t^l| \leq K \quad (8)$$

## 4 Experiments

### 4.1 Experimental setting

**Datasets:** We select four datasets for evaluation. The **CIFAR10-C** and **CIFAR100-C** [10] are small-scale corruption datasets, with 15 different common corruptions, each containing 10,000 corrupt images with 10/100 categories. For our evaluation in large-scale datasets, we opt for **ImageNet-C** [10], which also contains 15 different corruptions, each with 50,000 corrupt images in 1000 categories. Additionally, **ImageNet-D** [63] is a style-transfer dataset, offering 6 domain shifts, each consisting of 10,000 images selected in 109 classes.

**Implementation Details:** We follow the continual TTA setting [29, 10] to evaluate TTA performance under long-term adaptation, where the target domain undergoes continuous changes. For CIFAR10-C and CIFAR100-C, we use a batch size of 200 and the annotation percentage of 3%, with respectively employed pre-trained WideResNet-28 [47] and ResNeXt-29 [42] models. For ImageNet-C and ImageNet-D, we use a batch size of 64 for adaptation, and the annotation percentage is 3.2% of the total testing samples, with the ResNet-50 [10] pretrained model. For unsupervised training, we adopt the optimizer for the

respective methods presented in the original paper. For supervised training, we use Adam optimizer, with a  $1e-5$  learning rate for all methods throughout all datasets. We consider seven distinct values for each hyper-parameter category regarding model selection. We defer more detailed experimental settings to the appendix.

## 4.2 Evaluations on HILTTA

**Evaluation of Active Learning & Model Selection Strategies:** We report the classification error on the four datasets in Tab. 1. Each method is specified by two attributes. The “**Active Learning**” attribute indicates the sample selection method for additional human annotation. The “**Model Selection**” attribute indicates whether the method enables hyper-parameter selection proposed in Sec. 3.2. We use TENT [40] as an off-the-shelf TTA method. For methods that do not enable “Model Selection”, we report three results, the worst (**Worst**), average (**Avg.**), and best (**Best**). The worst or best results are obtained by a fixed hyper-parameter trained with which the model exhibits the worst or best overall accuracy. The average results are obtained by averaging the overall accuracy across the models trained upon all candidate hyper-parameters. We make the following observations from the results in Tab. 1. i) Without additional annotation (TENT) the worst and average performance could vary substantially (best 62.96% v.s. worst 95.23% on ImageNet-C). The results suggest the sensitivity to hyper-parameter remains a major challenge. ii) With additional annotation (TENT w/ HIL), we first notice that applying active learning alone consistently improves over fully unsupervised adaptation in terms of worst, average and best results. iii) When model selection is further applied, the hyper-parameter is automatically chosen, resulting in a single error rate. We witness that for all active learning methods, our model selection strategy achieves significant improvement from the average error rate. In many cases, we could even surpass the best result. iv) Finally, our proposed K-Margin selection strategy combined with model selection almost outperforms all other active learning techniques, suggesting the effectiveness of balancing active learning and model selection for HILTTA.

	Active Learning	Model Select.	ImageNet-C			ImageNet-D			CIFAR100-C			CIFAR10-C		
Source	×	×	Worst	Avg.	Best	Worst	Avg.	Best	Worst	Avg.	Best	Worst	Avg.	Best
TENT [40]	×	×	95.23	82.02	62.96	83.54	58.98	52.93	94.26	46.44	32.75	71.22	43.51	18.14
TENT w/ HIL	Random	×	95.04	67.08 (+6.05) 59.42 (+13.71)	59.60	79.15	55.01 (+4.81) 49.56 (+10.26)	49.59	94.26	50.70 (-0.01) 31.50 (+19.19)	30.87	64.61	24.91 (+2.86) 17.80 (+9.97)	16.84
	Entropy [40]	×	95.23	70.47 (+2.66) 60.45 (+12.68)	60.79	82.39	56.27 (+3.55) 49.48 (+10.34)	49.85	94.37	51.33 (-0.64) 32.78 (+17.91)	30.18	29.46	18.45 (+9.32) 15.82 (+11.95)	15.77
	K-Center [40]	×	94.49	69.90 (+3.23) 60.56 (+12.57)	60.73	80.15	56.40 (+3.42) 50.60 (+9.22)	50.83	94.56	53.08 (-2.39) 33.25 (+17.44)	32.08	60.62	25.92 (+1.85) 17.97 (+9.80)	17.81
	VeSSAL [40]	×	93.82	71.51 (+1.62) 62.37 (+10.76)	62.78	79.06	54.91 (+4.91) 49.56 (+10.26)	49.65	94.34	51.20 (-0.51) 32.89 (+17.80)	31.59	59.06	24.41 (+3.36) 17.81 (+9.96)	17.15
	ASE [40]	×	93.57	68.85 (+4.28) 60.52 (+12.61)	60.66	78.32	54.25 (+5.57) 53.08 (+6.74)	49.35	94.35	48.19 (+2.50) 31.16 (+17.53)	30.53	70.23	25.36 (+2.41) 17.49 (+10.28)	17.04
	SimATTA [40]	×	94.59	69.09 (+4.04) 60.46 (+12.67)	60.71	79.99	55.25 (+4.57) 49.59 (+10.23)	49.89	94.64	48.70 (+1.99) 31.23 (+19.46)	30.36	31.28	19.35 (+8.42) 16.95 (+10.82)	16.39
	K-Margin (OURS)	✓	94.98	68.13 (+5.00) 58.35 (+14.78)	58.49	76.27	53.77 (+6.05) 48.74 (+11.08)	48.55	94.75	49.37 (+1.32) 30.53 (+20.16)	30.11	27.81	18.21 (+9.56) 15.87 (+11.90)	15.75

Table 1: Evaluation under HILTTA with average classification error (lower is better). ‘Worst’, ‘Avg.’, and ‘Best’ denote the worst, average, and best performances, respectively, with the candidate hyper-parameter pool  $\Omega$ . The performance improvement by **Active Learning** and **Model Selection** is denoted within brackets as  $(\delta)$ .

**Evaluation under Alternative TTA Methods:** Moreover, we investigate various off-the-shelf TTA methods in Tab. 2. Employing our proposed K-Margin as the sample selection method, we consistently observe enhancements for all off-the-shelf TTA methods when paired with our HIL model selection and learning strategies. These findings advocate for our



active learning and model selection approach regardless of TTA methods. Importantly, even the simplest baseline, TENT, achieves comparable results to state-of-the-art TTA methods under HILTTA. The results suggest exploiting small amount of labeled data is very effective for TTA and the margin between different TTA methods are smaller than expected when equipped with human-in-the-loop.

TTA Methods	A.L.	M.S.	ImageNet-C			ImageNet-D			CIFAR100-C			CIFAR10-C		
			Worst	Avg.	Best	Worst	Avg.	Best	Worst	Avg.	Best	Worst	Avg.	Best
TENT [10]	×	×	95.23	73.13	62.96	83.54	59.82	52.93	94.26	50.69	32.75	71.22	27.77	18.14
	✓	×	94.98	68.13 (+5.00)	58.49	76.27	53.77 (+6.05)	48.55	94.75	49.37 (+1.32)	30.11	27.81	18.21 (+9.56)	15.75
	✓	✓		58.35 (+14.78)			48.74 (+11.08)			30.53 (+20.16)			15.87 (+11.90)	
PL [11]	×	×	89.78	81.48	67.75	63.06	56.59	52.45	37.31	34.67	32.76	19.95	19.11	18.54
	✓	×	79.14	70.30 (+11.18)	62.15	50.93	49.25 (+7.34)	48.15	32.08	30.85 (+3.82)	29.93	17.02	16.67 (+2.44)	16.45
	✓	✓		61.60 (+19.88)			49.01 (+7.58)			30.82 (+3.85)			16.97 (+2.14)	
SHOT [12]	×	×	99.18	79.56	64.68	91.51	64.51	53.69	90.72	43.89	32.90	52.87	23.22	17.26
	✓	×	99.29	74.49 (+5.07)	59.30	90.86	58.19 (+6.32)	48.37	87.30	41.05 (+2.84)	30.51	21.27	16.68 (+6.54)	15.66
	✓	✓		60.66 (+18.90)			48.98 (+15.53)			31.13 (+12.76)			15.78 (+7.44)	
EATA [13]	×	×	99.81	70.85	57.92	94.68	60.89	52.00	44.89	34.57	31.32	39.28	21.66	17.14
	✓	×	99.29	68.36 (+2.49)	54.37	94.75	56.93 (+3.96)	47.88	42.10	32.42 (+2.15)	29.51	25.06	17.82 (+3.84)	15.69
	✓	✓		56.75 (+14.10)			49.17 (+11.72)			30.43 (+4.14)			15.79 (+5.87)	
SAR [14]	×	×	90.60	70.70	62.20	56.19	53.37	51.72	39.00	33.84	31.90	20.22	19.10	17.45
	✓	×	89.03	64.81 (+5.89)	58.22	49.79	48.64 (+4.73)	47.50	32.24	30.63 (+3.21)	29.67	17.14	16.60 (+2.50)	15.63
	✓	✓		58.91 (+11.79)			50.02 (+3.35)			30.00 (+3.84)			16.87 (+2.23)	
RMT [15]	×	×	98.77	72.28	60.45	88.80	58.92	50.14	38.35	32.18	30.16	29.36	19.75	16.66
	✓	×	98.50	69.87 (+2.41)	56.67	87.96	55.51 (+3.41)	46.12	37.68	31.26 (+0.92)	29.02	27.04	18.35 (+1.40)	15.80
	✓	✓		58.26 (+14.02)			46.28 (+12.64)			29.41 (+3.38)			16.45 (+3.30)	

Table 2: Evaluation of different off-the-shelf TTA methods with K-Margin selection method under HILTTA protocol.

### 4.3 Ablation & Additional Study

**Unveiling the Impact of Individual Components:** We conduct a comprehensive ablation analysis using TENT as the off-the-shelf TTA method in Tab. 3. Compared with not adapting to testing data stream, fine-tuning with only the unsupervised training loss (Unsup. Train) could improve the performance, as expected. When human annotation is introduced, using the cross-entropy loss  $\mathcal{H}_{ce}$  as validation objective (CE Valid.) does not guarantee a consistent improvement. As discussed in [18], this can be attributed to the challenges posed by the min-max equilibrium optimization problem across time, resulting in a notable performance decline. Incorporating additional anchor regularization for model selection (referred to as Anchor Reg.) consistently improves performance beyond the average error rate of the original TENT. This underscores the necessity of stronger regularization for model selection to achieve overall good TTA performance. Additionally, integrating EMA smoothing (EMA Smooth.) of validation loss and supervised training with labeled data (referred to as Super. Train) both contribute positively to enhancing TTA performance.

Remark	Unsup. Train	CE Valid.	Anchor Reg.	EMA Smooth.	Super. Train	Error Rate (%) ↓			
						ImageNet-C	ImageNet-D	CIFAR100-C	CIFAR10-C
Source	-	-	-	-	-	82.02	58.98	46.44	43.51
TENT	✓	-	-	-	-	73.13	59.82	54.97	27.77
w/ HIL	✓	✓	-	-	-	90.52	62.66	67.82	21.36
w/ HIL	✓	✓	✓	-	-	65.95	52.87	47.55	17.79
w/ HIL	✓	✓	✓	✓	-	62.61	52.61	34.18	17.79
w/ HIL	✓	✓	✓	✓	✓	<b>58.35</b>	<b>48.74</b>	<b>30.53</b>	<b>15.87</b>

Table 3: Ablation study of HILTTA with TENT [10] as off-the-shelf TTA method.

**Evaluation of Alternative Model Selection Strategies:** We further compare our approach with existing model selection strategies. Entropy [17], InfoMax [18], and MixVal [13] represent the state-of-the-art in model selection methods for Unsupervised Domain Adaptation. For the Oracle model selection strategy for online TTA, referred to as PitTTA [18], leverages all labels within the streaming test dataset  $\mathcal{D}_t$  to conduct model selection based on accuracy comparison. The results in Tab. 4 reveal that our proposed methods consistently outperform



Strategy	Error Rate (%) ↓				Avg.
	ImageNet-C	ImageNet-D	CIFAR100-C	CIFAR10-C	
Fixed Worst	94.98	76.27	94.75	27.81	73.45
Fixed Best*	58.49	48.55	30.11	15.75	38.23
Entropy [■]	94.65	73.95	94.11	26.66	72.34
InfoMax [■]	94.56	77.00	93.14	28.81	73.38
MixVal [■]	92.98	68.20	92.23	19.64	68.26
PitTTA [■]	<u>60.75</u>	<u>47.95</u>	<u>47.99</u>	<u>16.23</u>	<u>43.23</u>
HILTTA (Ours)	<b>58.35</b>	<b>48.74</b>	<b>30.53</b>	<b>15.87</b>	<b>38.37</b>

Table 4: Comparison of different model selection strategies. \* indicate upper bound with fixed hyper-parameter

alternative model selection approaches, yielding comparable or even superior performance when compared to the best outcomes achieved with fixed hyper-parameter choices.

**Computation Efficiency:** We conducted empirical studies to measure the wall-clock time of both the inference and adaptation steps in HILTTA with results in Tab. 5. In this setup, we only perform human-in-the-loop annotation for every N batches on the testing data stream. The inference time required is fixed for all methods and the adaptation time varies. We demonstrate that the additional model selection procedure significantly decreases the error rate (27.77%  $\rightarrow$  15.87%) with 9 times overall time required (1ms v.s. 9.1ms). More importantly, the overall time required can be further reduced by conducting sparser human annotation (larger N). With N=10, we witness a 10% absolute error rate decrease (27.77%  $\rightarrow$  17.13%) with only 2.8 times computation time. Considering annotating a single image would cost 3000 ms to 5000 ms, the adaptation time is considered to be negligible.

	w/o HIL	w/ HIL N=1	w/HIL N=3	w/HIL N=5	w/HIL N=10
Error Rate (%)	27.77	15.87	15.98	16.43	17.13
Inference Time (ms/sample)	0.40	0.40	0.40	0.40	0.40
Adaptation Time (ms/sample)	0.60	8.70	3.50	2.60	1.40

Table 5: Computation efficiency under different human intervention frequencies.

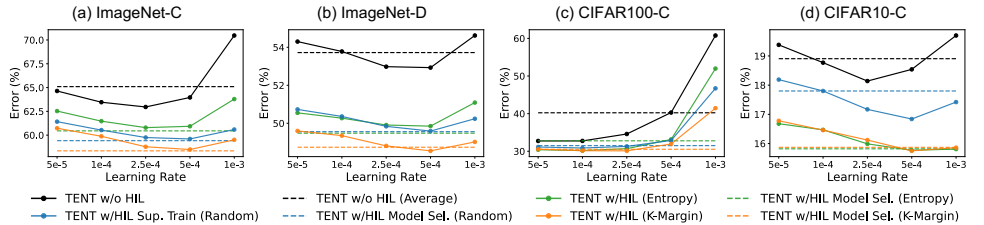


Figure 2: Performance of TENT[■] with and without HIL. Bold lines represent the performance with different hyper-parameter values, while dashed lines indicate the performance with model selection.

**Detailed Analysis of Performance:** We provide more detailed analysis against the selection of hyper-parameters. In particular, we investigate the performance of TENT with and without HIL and plot the results in Fig. 2. TENT w/o HIL and TENT w/o HIL (Average) refer to applying TENT without additional annotation and the average error rate respectively. TENT w/HIL Sup.Train (Random/Entropy/K-Margin) and TENT w/HIL Model Sel. (Random/Entropy/K-Margin) refer to augmenting TENT with supervised training on Random/Entropy/K-Margin labeled testing data and our proposed model selection respectively. The accuracy w/ HIL consistently surpasses all w/o HIL. Furthermore, random and entropy selection are consistently less effective than our proposed K-Margin selection for model selection purposes. Crucially, our final HILTTA approach consistently achieves significantly better performance than the worst hyper-parameter, and on ImageNet-C, we even surpass the model using the best fixed hyper-parameter.

## 5 Conclusion

In this study, we presented a novel perspective towards human-in-the-loop test-time adaptation (HILTTA) by synergizing active learning and model selection. Beyond active learning consideration, we further treat the labeled data as a validation set to enable the smooth selection of hyper-parameters and a subset for supervised training. We developed regularization techniques to augment the validation loss. A novel sample selection strategy is also proposed for HILTTA. Then we integrate HILTTA to multiple sample selection methods and off-the-shelf TTA methods and witness consistent improvement jointly brought by active learning and model selection over choosing the worst hyper-parameter and average performance. These explorations could help the community rethink the way to exploit the limited annotation budget in TTA tasks.

## References

- [1] Eric Arazo, Diego Ortego, Paul Albert, Noel E O'Connor, and Kevin McGuinness. Pseudo-labeling and confirmation bias in deep semi-supervised learning. In *Proceedings of 2020 International Joint Conference on Neural Networks*, pages 1–8. IEEE, 2020.
- [2] Jordan T Ash, Chicheng Zhang, Akshay Krishnamurthy, John Langford, and Alekh Agarwal. Deep batch active learning by diverse, uncertain gradient lower bounds. In *Proceedings of International Conference on Learning Representations*, 2020.
- [3] Yijin Chen, Xun Xu, Yongyi Su, and Kui Jia. Stfar: Improving object detection robustness at test-time by self-training with feature alignment regularization. *arXiv preprint arXiv:2303.17937*, 2023.
- [4] Francesco Croce, Maksym Andriushchenko, Vikash Sehwal, Edoardo Debenedetti, Nicolas Flammarion, Mung Chiang, Prateek Mittal, and Matthias Hein. Robustbench: a standardized adversarial robustness benchmark. In *Thirty-fifth Conference on Neural Information Processing Systems Datasets and Benchmarks Track (Round 2)*, 2021.
- [5] Jia Deng, Wei Dong, Richard Socher, Li-Jia Li, Kai Li, and Li Fei-Fei. Imagenet: A large-scale hierarchical image database. In *Proceedings of IEEE conference on computer vision and pattern recognition*, pages 248–255, 2009.
- [6] Mario Döbler, Robert A Marsden, and Bin Yang. Robust mean teacher for continual and gradual test-time adaptation. In *Proceedings of the IEEE/CVF Conference on Computer Vision and Pattern Recognition*, pages 7704–7714, 2023.
- [7] Yarin Gal and Alex Kendall. Deep bayesian active learning with image data. In *Proceedings of the International Conference on Machine Learning*, 2017.
- [8] Yaroslav Ganin and Victor Lempitsky. Unsupervised domain adaptation by backpropagation. In *Proceedings of International conference on machine learning*, pages 1180–1189, 2015.
- [9] Taesik Gong, Jongheon Jeong, Taewon Kim, Yewon Kim, Jinwoo Shin, and Sung-Ju Lee. NOTE: Robust continual test-time adaptation against temporal correlation. In *Proceedings of Advances in Neural Information Processing Systems (NeurIPS)*, 2022.

- [10] Shurui Gui, Xiner Li, and Shuiwang Ji. Active test-time adaptation: Theoretical analyses and an algorithm. In *Proceedings of International Conference on Learning Representations*, 2024.
- [11] Kaiming He, Xiangyu Zhang, Shaoqing Ren, and Jian Sun. Deep residual learning for image recognition. In *Proceedings of the IEEE conference on computer vision and pattern recognition*, pages 770–778, 2016.
- [12] Dan Hendrycks and Thomas Dietterich. Benchmarking neural network robustness to common corruptions and perturbations. In *Proceedings of International Conference on Learning Representations*, 2018.
- [13] Dapeng Hu, Jian Liang, Jun Hao Liew, Chuhui Xue, Song Bai, and Xinchao Wang. Mixed samples as probes for unsupervised model selection in domain adaptation. In *Proceedings of Advances in Neural Information Processing Systems (NeurIPS)*, 2023.
- [14] Yusuke Iwasawa and Yutaka Matsuo. Test-time classifier adjustment module for model-agnostic domain generalization. *Proceedings of Advances in Neural Information Processing Systems*, 34:2427–2440, 2021.
- [15] Ronald Kemker, Marc McClure, Angelina Abitino, Tyler Hayes, and Christopher Kanan. Measuring catastrophic forgetting in neural networks. In *Proceedings of the AAAI conference on artificial intelligence*, volume 32, 2018.
- [16] Jannik Kossen, Sebastian Farquhar, Yarin Gal, and Tom Rainforth. Active testing: Sample-efficient model evaluation. In *Proceedings of International Conference on Machine Learning*, pages 5753–5763, 2021.
- [17] Jannik Kossen, Sebastian Farquhar, Yarin Gal, and Thomas Rainforth. Active surrogate estimators: An active learning approach to label-efficient model evaluation. volume 35, pages 24557–24570, 2022.
- [18] Dong-Hyun Lee et al. Pseudo-label: The simple and efficient semi-supervised learning method for deep neural networks. In *Workshop on challenges in representation learning, ICML*, volume 3, page 896, 2013.
- [19] Jae-Hong Lee and Joon-Hyuk Chang. Continual momentum filtering on parameter space for online test-time adaptation. In *Proceedings of International Conference on Learning Representations*, 2024.
- [20] Yushu Li, Xun Xu, Yongyi Su, and Kui Jia. On the robustness of open-world test-time training: Self-training with dynamic prototype expansion. In *Proceedings of the IEEE/CVF International Conference on Computer Vision*, pages 11836–11846, 2023.
- [21] Zhizhong Li and Derek Hoiem. Learning without forgetting. *IEEE transactions on pattern analysis and machine intelligence*, 40(12):2935–2947, 2017.
- [22] Jian Liang, Dapeng Hu, and Jiashi Feng. Do we really need to access the source data? source hypothesis transfer for unsupervised domain adaptation. In *Proceedings of International conference on machine learning*, pages 6028–6039, 2020.

- [23] Jian Liang, Dapeng Hu, Yunbo Wang, Ran He, and Jiashi Feng. Source data-absent unsupervised domain adaptation through hypothesis transfer and labeling transfer. *IEEE Transactions on Pattern Analysis and Machine Intelligence*, 44(11):8602–8617, 2021.
- [24] Hanxiao Liu, Karen Simonyan, and Yiming Yang. Darts: Differentiable architecture search. In *Proceedings of International Conference on Learning Representations*, 2018.
- [25] Yuejiang Liu, Parth Kothari, Bastien Van Delft, Baptiste Bellot-Gurlet, Taylor Mordan, and Alexandre Alahi. Ttt++: When does self-supervised test-time training fail or thrive? volume 34, pages 21808–21820, 2021.
- [26] Robert A Marsden, Mario Döbler, and Bin Yang. Universal test-time adaptation through weight ensembling, diversity weighting, and prior correction. In *Proceedings of the IEEE/CVF Winter Conference on Applications of Computer Vision*, pages 2555–2565, 2024.
- [27] Pietro Morerio, Jacopo Cavazza, and Vittorio Murino. Minimal-entropy correlation alignment for unsupervised deep domain adaptation. In *Proceedings of International Conference on Learning Representations*, 2018.
- [28] Kevin Musgrave, Serge Belongie, and Ser-Nam Lim. Benchmarking validation methods for unsupervised domain adaptation. *arXiv preprint arXiv:2208.07360*, 2022.
- [29] Shuaicheng Niu, Jiaxiang Wu, Yifan Zhang, Yaofo Chen, Shijian Zheng, Peilin Zhao, and Mingkui Tan. Efficient test-time model adaptation without forgetting. In *Proceedings of International conference on machine learning*, pages 16888–16905, 2022.
- [30] Shuaicheng Niu, Jiaxiang Wu, Yifan Zhang, Zhiquan Wen, Yaofo Chen, Peilin Zhao, and Mingkui Tan. Towards stable test-time adaptation in dynamic wild world. In *Proceedings of International Conference on Learning Representations*, 2023.
- [31] Xingchao Peng, Qinxun Bai, Xide Xia, Zijun Huang, Kate Saenko, and Bo Wang. Moment matching for multi-source domain adaptation. In *Proceedings of the IEEE/CVF international conference on computer vision*, pages 1406–1415, 2019.
- [32] Ori Press, Steffen Schneider, Matthias Kümmerer, and Matthias Bethge. Rdumb: A simple approach that questions our progress in continual test-time adaptation. In *Proceedings of Advances in Neural Information Processing Systems (NeurIPS)*, 2023.
- [33] Evgenia Rusak, Steffen Schneider, Peter Vincent Gehler, Oliver Bringmann, Wieland Brendel, and Matthias Bethge. Imagenet-d: A new challenging robustness dataset inspired by domain adaptation. In *ICML 2022 Shift Happens Workshop*, 2022.
- [34] Akanksha Saran, Safoora Yousefi, Akshay Krishnamurthy, John Langford, and Jordan T Ash. Streaming active learning with deep neural networks. *arXiv preprint arXiv:2303.02535*, 2023.
- [35] Ozan Sener and Silvio Savarese. Active learning for convolutional neural networks: A core-set approach. In *Proceedings of International Conference on Learning Representations*, 2018.
- [36] Claude Elwood Shannon. A mathematical theory of communication. *The Bell system technical journal*, 27(3):379–423, 1948.

- [37] Yongyi Su, Xun Xu, and Kui Jia. Revisiting realistic test-time training: Sequential inference and adaptation by anchored clustering. *Proceedings of Advances in Neural Information Processing Systems*, 35:17543–17555, 2022.
- [38] Yongyi Su, Xun Xu, and Kui Jia. Towards real-world test-time adaptation: Tri-net self-training with balanced normalization. In *Proceedings of the AAAI Conference on Artificial Intelligence*, volume 38, pages 15126–15135, 2024.
- [39] Yongyi Su, Xun Xu, Tianrui Li, and Kui Jia. Revisiting realistic test-time training: Sequential inference and adaptation by anchored clustering regularized self-training. *IEEE Transactions on Pattern Analysis and Machine Intelligence*, 2024.
- [40] Yu Sun, Xiaolong Wang, Zhuang Liu, John Miller, Alexei Efros, and Moritz Hardt. Test-time training with self-supervision for generalization under distribution shifts. In *Proceedings of International conference on machine learning*, pages 9229–9248, 2020.
- [41] Dequan Wang, Evan Shelhamer, Shaoteng Liu, Bruno Olshausen, and Trevor Darrell. Tent: Fully test-time adaptation by entropy minimization. In *Proceedings of International Conference on Learning Representations*, 2020.
- [42] Qin Wang, Olga Fink, Luc Van Gool, and Dengxin Dai. Continual test-time domain adaptation. In *Proceedings of the IEEE/CVF Conference on Computer Vision and Pattern Recognition*, pages 7201–7211, 2022.
- [43] Wei Wang, Zhun Zhong, Weijie Wang, Xi Chen, Charles Ling, Boyu Wang, and Nicu Sebe. Dynamically instance-guided adaptation: A backward-free approach for test-time domain adaptive semantic segmentation. In *Proceedings of the IEEE/CVF Conference on Computer Vision and Pattern Recognition*, 2023.
- [44] Saining Xie, Ross Girshick, Piotr Dollár, Zhuowen Tu, and Kaiming He. Aggregated residual transformations for deep neural networks. In *Proceedings of the IEEE conference on computer vision and pattern recognition*, pages 1492–1500, 2017.
- [45] Shiqi Yang, Yaxing Wang, Joost Van De Weijer, Luis Herranz, and Shangling Jui. Generalized source-free domain adaptation. In *Proceedings of the IEEE/CVF International Conference on Computer Vision*, pages 8978–8987, 2021.
- [46] Longhui Yuan, Binhui Xie, and Shuang Li. Robust test-time adaptation in dynamic scenarios. In *Proceedings of the IEEE/CVF Conference on Computer Vision and Pattern Recognition*, pages 15922–15932, 2023.
- [47] Sergey Zagoruyko and Nikos Komodakis. Wide residual networks. In *Proceedings of the British Machine Vision Conference*, 2016.
- [48] Hao Zhao, Yuejiang Liu, Alexandre Alahi, and Tao Lin. On pitfalls of test-time adaptation. In *Proceedings of International Conference on Machine Learning*, pages 42058–42080, 2023.

## Appendix

In this appendix, we first provide a detailed description of our HILTТА algorithm. We further present additional insights and analysis including performance evolution, selecting two hyper-parameters, additional labeling budgets, computation complexities, and comparison with additional methods. Finally, we provide more details of experiments.

### A Overall Algorithm for HILTТА

---

**Algorithm 1:** Human-in-the-Loop TТА
 

---

**Input** : Source Model  $\theta_0$ ; Candidate Hyper-parameters  $\Omega = \{\omega_m\}$ ; Testing Data Batches  $\{B_t\}$

**Output:** Predictions  $\hat{\mathcal{Y}} = \{\hat{y}_i\}$

**for**  $t = 1$  **to**  $T$  **do**

  # Make Predictions:

$\forall x_i \in B_t, \hat{y}_i = h(x_i; \theta^{t-1*}), \hat{\mathcal{Y}} = \hat{\mathcal{Y}} \cup \hat{y}_i$

  # Oracle Annotation:

  Select labeled subset  $B_t^l$  by Eq. 8

**for**  $m = 1$  **to**  $N_m$  **do**

    # Unsupervised Model Adaptation:

$\theta_m^* = \arg \min_{\theta} \frac{1}{N_b} \sum_{x_i \in B_t^u} \mathcal{L}_{tr}^u(h(x_i; \theta); \omega_m)$

  # Update Moving Average Validation Loss:

  Update  $\tilde{\mathcal{L}}_{val}^t$  by Eq. 6.

  # Model Selection by Eq. 6:

$\theta^{t*} = \arg \min_m \tilde{\mathcal{L}}_{val}^t(\theta_m^*)$

  # Supervised Model Adaptation:

$\theta^{t*} = \arg \min_{\theta} \frac{1}{N_b} \sum_{x_i, y_i \in B_t^l} \mathcal{L}_{tr}^l(h(x_i; \theta), y_i; \omega_m)$

**return** Predictions  $\hat{\mathcal{Y}}$ ;

---

We introduce two types of training losses for model updates and a validation loss for model selection. In the model selection stage, multiple candidate models are obtained by training with an unsupervised TТА training loss, denoted as  $\mathcal{L}_{tr}^u$ . The exact design of  $\mathcal{L}_{tr}^u$  follows the off-the-shelf TТА methods. Then we select the best candidate model  $\theta^{t*}$  by  $\arg \min_m \tilde{\mathcal{L}}_{val}^t(\theta_m^*)$ . After the model selection stage, we further update the model in a supervised manner by optimizing a cross-entropy loss, denoted as  $\mathcal{L}_{tr}^l$ . We finally present the overall algorithm for Human-in-the-Loop Test-Time Adaptation in Alg. 1.

### B Further Insights and Analysis Findings

#### B.1 Temporal Evolution Analysis of HILTТА

We present an analysis of the evolution of selected hyper-parameters over time. As shown in Fig. 3, the hyper-parameters selected by our HILTТА model selection method always hover

around the upper bound “Fixed Best” while competing methods deviate further away from the upper bound. The advantage is also reflected in the accumulated error plot. In particular, methods such as MixVal [13], are susceptible to catastrophic failure as they struggle to adapt to continuously changing domains.

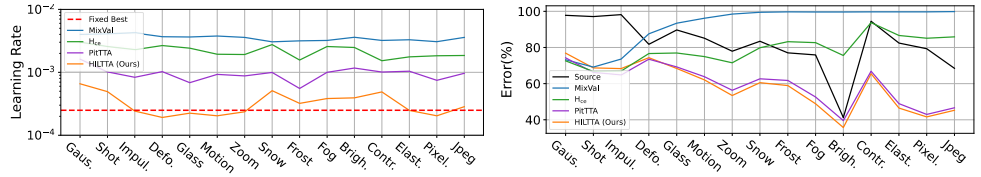


Figure 3: (Left) Average selected learning rate per corruption for TENT on ImageNet-C. (Right) Average error rate per corruption for TENT on ImageNet-C.

## B.2 Selecting Two Hyperparameters

In certain cases, there are more than one hyper-parameter should be selected. We evaluate HILTTA combined with PL [18] on CIFAR10-C by selecting two hyper-parameters, i.e. the self-training threshold and learning rate. As shown in Tab. 6, our HILTTA achieves the 3rd best result among 25 candidate hyper-parameter sets. The results suggest our method is agnostic to the number of hyper-parameters and can be utilized for real-world TTA tasks where an annotation budget is available.

LR/Threshold	0.1	0.2	0.4	0.6	0.8	AVG. Error	HILTTA (OURS)
1e-5	17.17	17.12	17.19	17.22	17.22	28.96	<b>16.41</b>
1e-4	17.08	17.10	17.01	17.13	17.04		
1e-3	16.99	16.76	16.54	16.49	16.43		
1e-2	<b>15.89</b>	<b>15.56</b>	20.29	23.69	23.56		
1e-1	22.41	81.89	88.64	88.89	88.78		

Table 6: Select two hyperparameters at the same time with PL on Cifar10-C, error rate is reported.

## B.3 Performance Under Different Labeling Budgets

We investigate the effectiveness of HILTTA under different annotation budgets. Specifically, we vary the annotation ratio from 0% to 10%. As shown in Tab. 7, with the increase of annotation budget, we observe consistent improvement in error rate for all off-the-shelf TTA methods. Importantly, naive methods, e.g. TENT, exhibit superior performance at higher labeling budget than more sophisticated ones, e.g. EATA, SAR and RMT. This suggests that limited labeled data could substantially ease the challenges of TTA.

## B.4 Comparing Adaptation Time & Annotation Time

We carried out empirical studies by measuring the wall-clock time lapses of the inference step (Inference Time), adaptation step (Adaptation Time), and human annotation (Annotation Time) per sample. In specific, the "Inference Time" refers to the time-lapse of pure



Budget	TENT	PL	SHOT	EATA	SAR	RMT
0%	27.77	19.11	23.22	19.57	19.10	19.75
1%	17.03	18.09	16.61	17.27	18.06	17.36
2%	16.35	17.30	16.21	16.81	17.30	16.41
3%	15.87	16.97	15.78	16.40	16.87	16.45
5%	15.13	16.45	15.44	15.83	16.12	16.78
10%	14.68	15.66	14.78	15.01	15.41	16.85

Table 7: Performance under different labeling budgets on CIFAR10-C, average error rates are reported.

forward pass, the "Adaption Time" refers to the time-lapse of backpropagation and weights update, and "Annotation Time" refers to the estimated time lapse required for human to annotate images at a 3% labeling rate. We evaluate under three categories of annotation cost, i.e. 2 sec/sample, 5 sec/sample, and 10 sec/sample. As seen from Tab. 8, despite the adaptation time being higher than the inference time (8.7 ms v.s. 0.4 ms), the annotation time is the most expensive step. These results suggest model selection and adaptation do not slow down the throughput under the HILTТА protocol.

	Inference	Adaptation	Annotation (2 sec/sample)	Annotation (5 sec/sample)	Annotation (10 sec/sample)
Time (ms/sample)	0.40	8.70	60.00	150.00	300.00

Table 8: Comparing HILTТА and annotation time consuming with a 3% label rate on CIFAR10-C

## B.5 Computation Complexity of Competing Methods

We conclude that existing stream-based active learning (VeSSAL [14]) and active TTA (SimATTA [15]) are inherently more computationally expensive than HILTТА due to the following reasons. First, VeSSAL adopts gradient embedding, i.e.  $g(x_i) = \partial l(f(x_i; \theta), y_i) / \partial \theta_L$ , where  $\theta_L \in \mathbb{R}^{K \times D}$  refers to the classifier weights. This results in a very high dimensional gradient embedding  $g(x_i) \in \mathbb{R}^{D \times K}$ . The probability of labeling a sample  $p_i$  involves calculating the inverse of covariance matrix, i.e.  $p_i \propto g(x_i)^\top \hat{\Sigma}^{-1} g(x_i)$ , s.t.  $\hat{\Sigma} = \sum_{x_i \in \mathcal{B}} g(x_i) g(x_i)^\top \in \mathbb{R}^{DK \times DK}$ . Hence, **VeSSAL can hardly deal with classification tasks with a large number of classes**, e.g. ImageNet, where  $K$  is large and calculating a large matrix inverse is inherently time-consuming. Second, SimATTA employs a K-Means clustering algorithm for the selection of samples to annotate. Since **K-Means is an iterative approach** the computation cost of SimATTA is relatively high as well. In contrast, our proposed sample selection is built upon K-Center clustering which sequentially selects the sample with the highest distance to cluster centers (greedy algorithm), the **computation cost is significantly lower than VeSSAL and SimATTA**. An empirical study in Tab. 9 reveals that our method is at least 3 times faster than VeSSAL and SimATTA in Adaptation Time.

Methods	Error	Adaptation Time (ms/sample)
VeSSAL	24.41	26.90
SimATTA	17.66	22.50
HILTТА (OURS)	<b>15.87</b>	<b>8.70</b>

Table 9: Error rate and adaptation wall time comparing to different methods on CIFAR10-C dataset

## B.6 Studies for Regularization in HILTTA

We argue that proposed anchor regularization and EMA smoothing for model selection in HILTTA prevent the model from overly adapting to local data distribution on the testing data stream. Removing them may help adaptation to a single domain but harm the performance of future domains. As shown in Tab. 10, in the continual TTA setting, model selection without regularization is much worse than the one with regularization (17.25% v.s. 15.87%), suggesting regularization is necessary for continual TTA.

Regularization	Gaussian	Shot	Impulse	Defocus	...	Jpeg	AVG.
Without	<b>25.04</b>	20.23	28.57	12.22	...	19.37	17.25
With	25.93	<b>20.13</b>	<b>27.49</b>	<b>11.59</b>	...	<b>18.26</b>	<b>15.87 (+1.38)</b>

Table 10: Comparison between w/ and w/o regularization for HILTTA with TENT on Cifar10-C. error rates are reported.

## B.7 Comparing with Knowledge Distillation and Ensemble Learning

We carried out additional experiments by comparing with ensemble learning and multi-teacher knowledge distillation methods. Specifically, for ensemble learning, we average the posterior predicted by each candidate model and make a prediction with the average posterior. For multi-teacher knowledge distillation, we use the pseudo label predicted by the ensemble model for self-training. As observed from Tab. 11, both ensemble learning and multi-teacher knowledge distillation yield inferior results than HILTTA. This is most likely caused by incorporating poor candidate models (ensemble learning) and using poor pseudo labels for self-training, i.e. learning from noisy labeled data (multi-teacher knowledge distillation).

Method	Average Performance on all candidate model	Ensemble Learning	Multi-teacher Knowledge Distillation	HILTTA (OURS)
Error	27.77	19.48	26.42	<b>15.87</b>

Table 11: Comparison with Ensemble Learning and Knowledge Distillation with TENT on CIFAR10-C.

## B.8 Random Batchsizes

We recognize that in certain scenarios, test data may arrive inconsistently and intermittently. Results from Tab. 12 demonstrate that our proposed HILTTA framework is adaptable to such varying batchsize. At each iteration, we vary the batchsize randomly among the choices [50, 100, 150, 200]. This versatility leads to even greater improvements compared to fixed batch size. This enhanced performance stems from the fact that the optimal hyperparameter values vary with different batch sizes, thus benefiting significantly from our adaptive model selection approach.

Batchsize	w/o HIL	HILTTA
200	27.77	<b>15.87 (+11.90)</b>
Random choose from [50,100,150,200]	35.89	<b>16.39 (+19.50)</b>

Table 12: Adaptation error with various batchsize with TENT on CIFAR10-C.

## B.9 Ablation Study with RMT

We have conducted wider experiments to analyze the ablation study with RMT [9] as the off-the-shelf TTA method in Tab. 13 exhibits a consistent trend with the findings presented in the manuscript, providing additional support for our analysis and demonstrating the effectiveness of our proposed approach.

Remark	Unsup. Train.	CE Valid.	Anchor regular.	EMA Smooth.	Super. Train.	Error (%) ↓			
						ImageNet-C	ImageNet-D	CIFAR100-C	CIFAR10-C
Source	-	-	-	-	-	82.02	58.98	46.44	43.51
RMT	✓	-	-	-	-	72.28	58.92	32.18	19.75
w/ HIL	✓	✓	-	-	-	98.34	49.98	36.28	24.94
w/ HIL	✓	✓	✓	-	-	67.98	51.40	31.53	19.18
w/ HIL	✓	✓	✓	✓	-	61.33	50.23	30.75	17.33
w/ HIL	✓	✓	✓	✓	✓	<b>58.26</b>	<b>46.28</b>	<b>29.41</b>	<b>16.45</b>

Table 13: Ablation study of HILTTA. Average classification error is reported for combing with RMT.

## C Experiment Details

### C.1 Detailed Settings for Datasets

Following prior works [6, 29, 30], we perform continual test time adaptation in the following datasets, detailed in follows.

**CIFAR10-C** [32] is a small-scale corruption dataset, with 15 different common corruptions, each containing 10,000 corrupt images of dimension (3, 32, 32) with 10 categories. We evaluate severity level 5 images, with "Gaussian → shot → impulse → defocus → glass → motion → zoom → snow → frost → fog → brightness → contrast → elastic → pixelate → jpeg" sequence.

**CIFAR100-C** [32] is a small-scale corruption dataset, with 15 different common corruptions, each containing 10,000 corrupt images of dimension (3, 32, 32) with 100 categories. We evaluate severity level 5 images, with "Gaussian → shot → impulse → defocus → glass → motion → zoom → snow → frost → fog → brightness → contrast → elastic → pixelate → jpeg" sequence.

**ImageNet-C** [32] is a large-scale corruption dataset, with 15 different common corruptions, each containing 50,000 corrupt images of dimension (3, 224, 224) with 1000 categories. We evaluate the first 5,000 samples with severity level 5 following [9]. The domain sequence is "Gaussian → shot → impulse → defocus → glass → motion → zoom → snow → frost → fog → brightness → contrast → elastic → pixelate → jpeg".

**ImageNet-D** [33], as a large-scale style-transfer dataset, is built upon DomainNet [34], which encompasses 6 domain shifts (clipart, infograph, painting, quickdraw, real, and sketch). The dataset focuses on samples belonging to the 164 classes that overlap with ImageNet. Following [36], we specifically select all classes with a one-to-one mapping from DomainNet to ImageNet, resulting in a total of 109 classes and excluding the quickdraw domain due to the challenge of attributing many examples to a specific class. After processing, it contains 5 domain shifts with each 10,000 images selected in 109 classes. The domain sequence is "clipart → infograph → painting → real → sketch".

## C.2 Detailed Settings for Comparing Methods

We mainly follow the official implementation of each method and use the same optimization strategy. But in certain cases, such as transferring from another protocol, we make minor changes to the configuration.

**Source** serves as the baseline for inference performance without any adaptation.

**TENT [49]**. It focuses on updating batch normalization layers through entropy minimization. We follow the official implementation<sup>1</sup> of TENT to update BN parameters.

**PL [18]**. We implement self-supervised training on unlabeled data updating all parameters by cross-entropy with an entropy threshold  $E = \theta \times \log(\#class)$ . For CIFAR10-C and CIFAR100-C, we use an SGD optimizer with a 1e-3 learning rate, while an SGD optimizer with a 2.5e-5 learning rate for the rest.

**SHOT [22]**. It freezes the linear classifier and trains the feature extractor by balancing prediction category distribution, coupled with pseudo-label-based self-training. We follow its official code<sup>2</sup> to update the feature extractor but remove the threshold. For CIFAR10-C and CIFAR100-C, we use an SGD optimizer with a 1e-3 learning rate, while an SGD optimizer with a 2.5e-5 learning rate.

**EATA [49]**. It adapts batch normalization layers using entropy minimization but introduces an additional fisher regularization term to prevent drastic parameter changes. We follow the official implementation<sup>3</sup> of EATA to update BN parameters. We hold 2000 fisher training samples and keep the entropy threshold  $E_0 = 0.4 \times \log(\#class)$ .

**SAR [50]**. It updates batch normalization layers with a sharpness-aware optimization approach. We mainly follow its official code<sup>4</sup>, but set  $e_0 = 0$  for CIFAR10-C and CIFAR100-C, preventing failure cases of frequently resetting the model’s weight.

**RMT [6]**. It adapts in a teacher-student mode, incorporating cross-entropy consistency loss and contrastive loss. We follow the official implementation<sup>5</sup>.

**ASE [17]**. It uses surrogate estimators to sample in a uncertainty distribution to sample with low bias. We follow its official implementation<sup>6</sup>.

**SIMATTA [10]**. As an active test-time adaptation method, it selects labeled samples through incremental clustering and updates the model by minimizing cross-entropy. To reduce the computational and memory cost of incremental clustering, we keep the maximum length of anchors to 50 in all experiments. For CIFAR10-C and CIFAR100-C, we set the lower entropy bound  $e_l$  to 0.005 and 0.01 for the higher entropy bound  $e_u$ . While for ImageNet-C and ImageNet-D, we set the lower entropy bound  $e_l$  to 0.2 and 0.4 for the higher entropy bound  $e_u$ .

**VeSSAL [34]**. As a stream-based active learning method, it uses volume sampling for streaming active learning. We also follow its official implementation<sup>7</sup>, using feature embedding for stream-based data selection.

<sup>1</sup><https://github.com/DequanWang/tent>

<sup>2</sup><https://github.com/tim-learn/SHOT>

<sup>3</sup><https://github.com/mr-eggplant/EATA>

<sup>4</sup><https://github.com/mr-eggplant/SAR>

<sup>5</sup><https://github.com/mariodoebler/test-time-adaptation>

<sup>6</sup><https://github.com/jlko/active-surrogate-estimators>

<sup>7</sup><https://github.com/asaran/VeSSAL>

### C.3 Hyper-parameter Choices for Model Selection

To achieve a fair and diverse validation process, we select three main kinds of hyper-parameters, i.e. threshold, loss coefficient, and learning rate. Detailed hyper-parameter settings along with the search space are available in Tab. 14.

TTA method	Hyper-parameter	Search Space
TENT [41]	Learning Rate $\eta$	{5e-5, 1e-4, 2.5e-4, 5e-4, 1e-3, 2.5e-3, 5e-3}
PL [18]	Entropy Threshold $\tau$	{0.05, 0.1, 0.2, 0.4, 0.6, 0.8, 1.0}
SHOT [27]	Loss Coefficient $\beta$	{0.1, 0.25, 0.5, 1.0, 2.5, 5.0, 10.0}
EATA [29]	Learning Rate $\eta$	{5e-5, 1e-4, 2.5e-4, 5e-4, 1e-3, 2.5e-3, 5e-3}
SAR [30]	Learning Rate $\eta$	{5e-5, 1e-4, 2.5e-4, 5e-4, 1e-3, 2.5e-3, 5e-3}
RMT [6]	Loss Coefficient $\lambda_{CL}$	{0.1, 0.25, 0.5, 1.0, 2.5, 5.0, 10.0}

Table 14: Overview of the TTA methods validated and their associated hyper-parameters